Perpendicular magnetic anisotropy in CoxMn4−xN (x = 0 and 0.2) epitaxial films and possibility of tetragonal Mn4N phase

Keita Ito, Yoko Yasutomi, Kazuki Kabara, Toshiki Gushi, Soma Higashikozono, Kaoru Toko, Masakiyo Tsunoda, and Takashi Suemasu

Citation: AIP Advances **6**, 056201 (2016); doi: 10.1063/1.4942548
View online: http://dx.doi.org/10.1063/1.4942548
View Table of Contents: http://scitation.aip.org/content/aip/journal/adva/6/5?ver=pdfcov
Published by the AIP Publishing

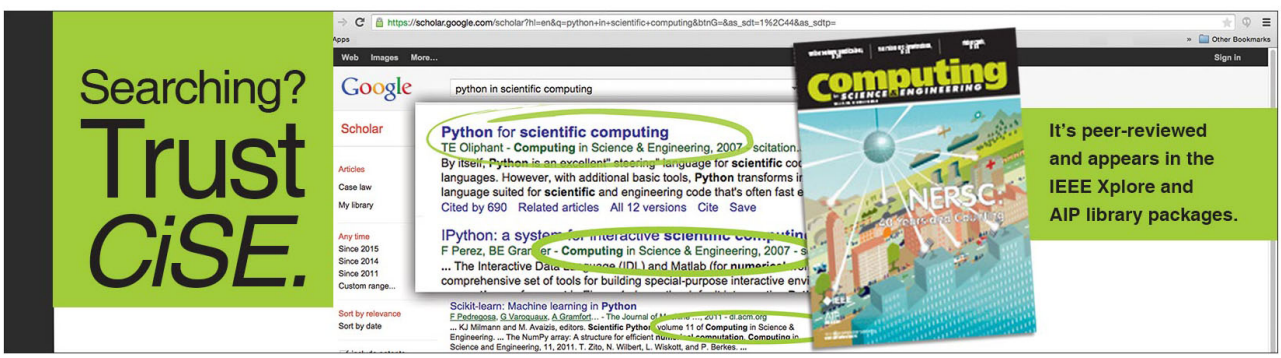

Perpendicular magnetic anisotropy in $Co_xMn_{4-x}N$ (x = 0 and 0.2) epitaxial films and possibility of tetragonal Mn_4N phase

Keita Ito,[1,2,3,a] Yoko Yasutomi,[1] Kazuki Kabara,[2] Toshiki Gushi,[1] Soma Higashikozono,[1] Kaoru Toko,[1] Masakiyo Tsunoda,[2] and Takashi Suemasu[1]

[1]*Institute of Applied Physics, Graduate School of Pure and Applied Sciences, University of Tsukuba, Tsukuba, Ibaraki 305-8573, Japan*

[2]*Department of Electronic Engineering, Graduate School of Engineering, Tohoku University, Sendai 980-8579, Japan*

[3]*Japan Society for the Promotion of Science (JSPS), Chiyoda, Tokyo 102-0083, Japan*

(Presented 12 January 2016; received 31 October 2015; accepted 11 November 2015; published online 18 February 2016)

We grow 25-nm-thick Mn_4N and $Co_{0.2}Mn_{3.8}N$ epitaxial films on $SrTiO_3$(001) by molecular beam epitaxy. These films show the tetragonal structure with a tetragonal axial ratio c/a of approximately 0.99. Their magnetic properties are measured at 300 K, and perpendicular magnetic anisotropy is confirmed in both films. There is a tendency that as the Co composition increases, an anisotropy field increases, whereas saturation magnetization and uniaxial magnetic anisotropy energy decrease. First-principles calculation predicts the existence of tetragonal Mn_4N phase. This explains the $c/a \sim 0.99$ in the Mn_4N films regardless of their film thickness and lattice mismatch with substrates used. [http://dx.doi.org/10.1063/1.4942548]

I. INTRODUCTION

To realize high-performance magnetic recording devices and spintronics devices, extensive search has been conducted on ferromagnetic materials possessing outstanding features such as a large spin polarization and perpendicular magnetic anisotropy (PMA). In particular, ferromagnetic materials which show both small saturation magnetization (M_S) and strong PMA have drawn increased interest as materials for spin-transfer torque magnetic random access memory[1] and current-driven domain wall motion nonvolatile memory.[2] Among such materials, we have focused much attention on anti-perovskite nitrides and their mixed crystals from both theory and experiments.[3–12] Mn_4N is one of the anti-perovskite ferrimagnetic nitrides, and PMA was reported for films grown on glass,[13] Si(001),[14] MgO(001),[15–19] and $SrTiO_3$(STO)(001)[16] substrates. Figure 1 shows the lattice structure of Mn_4N. One N atom is located at body center and Mn atoms are located at corner (I) site and face-centered (II) site of the cube.[3] Mn_4N bulk has a lattice constant of a_0 = 0.387 nm, and is ferrimagnetic metal (M_S = 182 emu/cm^3 at 77 K) with the Curie temperature of 745 K.[3] The magnetic moments of Mn atoms were evaluated to be 3.85 μ_B at I sites and −0.90 μ_B at II sites from the neutron diffraction measurement at 77 K,[3] where μ_B is the Bohr magneton. For Mn_4N thin films in Refs. 15–19, the in-plane lattice constant (a) and perpendicular lattice constant (c) were evaluated by x-ray diffraction (XRD), and the tetragonal structure ($c/a \sim 0.99$) was reported regardless of layer thickness and substrate used. It is considered that the origin of PMA in Mn_4N is ascribed to the in-plane tensile strain.[15–19] However, $c/a \sim 0.99$ and PMA were reported even in the Mn_4N film on MgO(001), in which misfit dislocations were observed immediately above

[a]Electronic mail: keita.ito.729@gmail.com

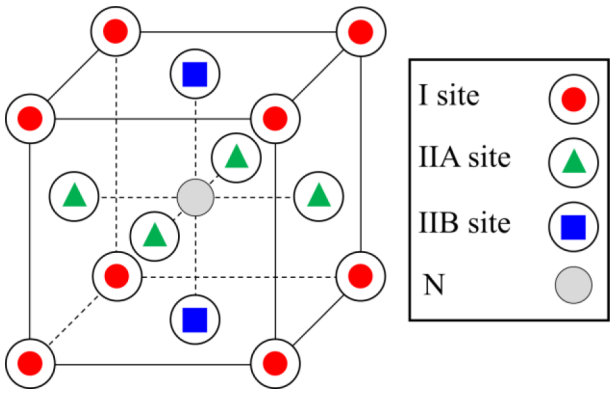

FIG. 1. Schematic of an anti-perovskite lattice structure.

the interface between the film and the substrate.[17] The lattice mismatch between them is −8.2%. It is reasonable to consider that tensile strain is not likely to remain in such films. Thus, the origin of the observed tetragonal Mn_4N films is an open question. In addition, despite a number of studies on anti-perovskite nitrides so far, there have been no reports on magnetic properties of single crystalline $Co_xMn_{4-x}N$ films. In this study, we evaluated the c/a ratio, electrical resistivity (ρ), M_S, and uniaxial magnetic anisotropy energy (K_u) in approximately 25-nm-thick Mn_4N and $Co_{0.2}Mn_{3.8}N$ epitaxial thin films grown on STO(001) substrates by molecular beam epitaxy (MBE). Our objective is to clarify the effect of Co substitution for Mn site on the magnetic properties of Mn_4N. In addition, we investigated the possibility of tetragonal Mn_4N phase using the first-principles calculation.

II. EXPERIMENTS AND CALCULATION

We grew approximately 25-nm-thick Mn_4N and $Co_{0.2}Mn_{3.8}N$ epitaxial films on STO(001) substrates at 450 ºC by MBE using solid sources of Co and Mn, and radio-frequency N plasma. The details of growth procedure are described in Ref. 16. The sample structures are Al/Mn_4N/STO and Al/$Co_{0.2}Mn_{3.8}N$/STO, where 10-nm-thick Al capping layers were deposited to prevent oxidation. We also prepared those without the Al capping layers for resistivity measurement. The crystalline quality of the grown films was characterized by reflection high-energy electron diffraction (RHEED) and out-of-plane (ω-2θ) XRD measurement. c/a of the films was deduced from x-ray reciprocal lattice mapping. We used Rutherford back scattering spectrometry and electron probe microanalyzer measurements to evaluate x in $Co_xMn_{4-x}N$. We also measured temperature dependences of ρ at temperatures from 10 to 300 K by four-point probe method. Magnetization versus magnetic field curves were measured by superconducting quantum interference device (SQUID) magnetometer at 300 K. External magnetic field (H) of −50 to 50 kOe was applied parallel and perpendicular to the film surface. To calculate M_S per unit volume, the grown layer thickness was determined from x-ray reflectivity and its area was deduced by a top-view photo. Magnetic torque (T) curves were measured at room temperature (RT) under H varied as 7.5, 9, 12, 15, 17, 19, 21, 23, or 25 kOe, by rotating the electromagnet clockwise (cw) and counterclockwise (ccw). The K_u values were deduced by so-called the 45°-torque method.[20] We performed the first-principles calculations on Mn_4N by using the Bader analysis[21] and the Vienna *ab initio* simulation package[22] (VASP) with the projected-augment wave pseudopotential[23] and a spin-polarized Perdew-Burke-Ernzerhof generalized gradient approximations and Perdew-Wang exchange-correlation function.[24] The convergence in the total electron energy (E_{tot}) was better than 10^{-7} eV/cell using the energy cut off of 400 eV. The k-points sampling of 11 × 11 × 11 were used for the calculation of the charge density with VASP. In the calculation, we assumed two types of Mn_4N, type A and type B. In type A Mn_4N, the spin magnetic moment (m_{spin}) of Mn atoms located at I sites is anti-parallel to that at both IIA and IIB sites. On the other hand, in type B Mn_4N, the m_{spin} at I sites is parallel to that at IIB sites and anti-parallel to that at IIA sites. We calculated the

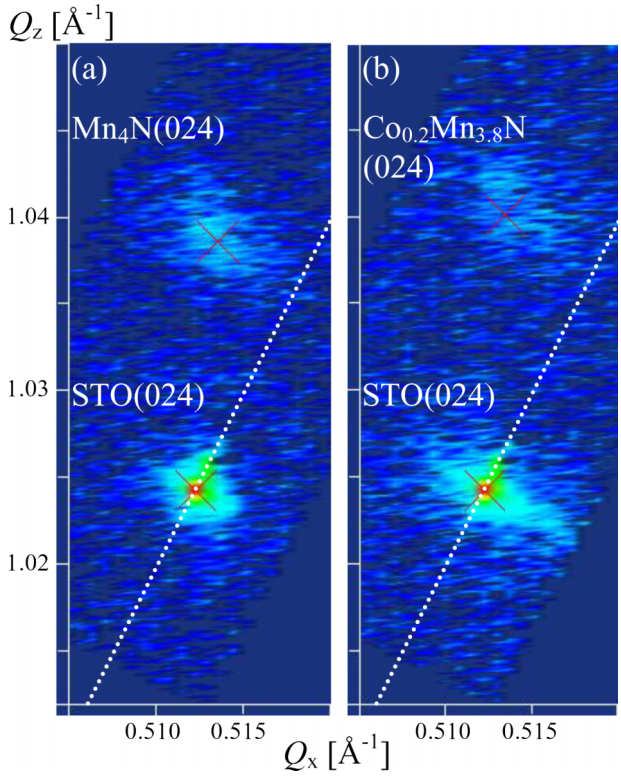

FIG. 2. X-ray reciprocal lattice mappings of (a) Mn_4N and (b) $Co_{0.2}Mn_{3.8}N$ films.

m_{spin} of each site and E_{tot} in both type A and type B Mn_4N by changing the c/a ratio with the fixed unit cell's volume a_0^3.

III. RESULTS AND DISCUSSION

Epitaxial growth of Mn_4N and $Co_{0.2}Mn_{3.8}N$ films was confirmed by c-axis-oriented XRD peaks such as (002) and (004) together with streaky RHEED patterns. Figures 2(a) and 2(b) show the reciprocal lattice mapping of STO(024) and $Co_xMn_{4-x}N$(024) (x = 0 and 0.2) spots, respectively. The white dotted line in the figures passes the origin of the reciprocal lattice map and the diffraction spot of STO(024). The diffraction spot of $Co_xMn_{4-x}N$(024) is located on the left side of the line in Figs. 2(a) and 2(b), meaning the tetragonal structure of the grown layers. The lattice constants (a = 0.389 nm and c = 0.385 nm) and the tetragonal axial ratio of $c/a \sim 0.99$ was obtained in both samples. The lattice constants of the Mn_4N layer was almost the same as those in Ref. 16 (a = 0.390 nm and c = 0.386 nm).

The resistivity ρ of the Mn_4N and $Co_{0.2}Mn_{3.8}N$ films decreased with decreasing temperature and became almost constant in the low temperature region. This is a typical behavior in metals. The ρ values at 10 and 300 K were 26 and 164 μΩ·cm in Mn_4N, and 79 and 166 μΩ·cm in $Co_{0.2}Mn_{3.8}N$, respectively. The larger ρ at low temperatures in $Co_{0.2}Mn_{3.8}N$ than in Mn_4N is likely caused by alloy scattering due to disordered arrangement of Co and Mn atoms, because ordered structures are probable only when x = 1, 2, or 3 in the $Co_xMn_{4-x}N$ system. The temperature dependence of ρ was already reported in Mn_4N films formed on MgO(001) by pulsed laser deposition (PLD)[17] and by MBE.[18] The ρ value of the Mn_4N film in the present work is slightly larger than that in Ref. 17, and is approximately 8 times larger than that in Ref. 18 at 300 K. We think that the difference of N content in the film may affect the magnitude of ρ.

Figures 3(a) and 3(b) show the magnetization curves of Mn_4N and $Co_{0.2}Mn_{3.8}N$ films measured by SQUID magnetometer. The hysteresis curve was clearly open when H was applied perpendicular

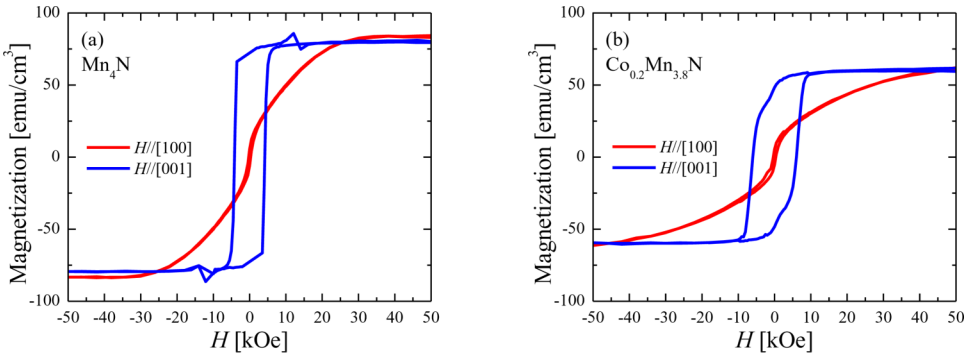

FIG. 3. Magnetization curves of (a) Mn_4N and (b) $Co_{0.2}Mn_{3.8}N$ films. The hysteresis was open when H was applied normal to the sample surface in both cases.

to the film in both samples, showing the occurrence of PMA. The anisotropy field (H_k) value of the $Co_{0.2}Mn_{3.8}N$ films was larger than that of the Mn_4N film. The M_S values of Mn_4N and $Co_{0.2}Mn_{3.8}N$ were 80 and 60 emu/cm^3, respectively, showing that M_S was reduced by the slight addition of Co into Mn_4N. This value is smaller than those already reported such as 145 emu/cm^3 in approximately 30-nm-thick Mn_4N on STO(001) formed by MBE,[16] and 157 emu/cm^3 in Mn_4N on MgO(001) grown by PLD.[17] It is reported that the value of M_S in Mn_4N changed depending on N_2 gas supply during the growth.[19] We speculate that the N vacancy may affect the M_S value in Mn_4N. In this experiment, we set the total deposition amount of 3*d* element and N_2 gas flow to be the same for the Mn_4N and $Co_{0.2}Mn_{3.8}N$ films. Therefore, the change in M_S between the two samples is attributed to the addition of Co. We performed first-principles calculations for $CoMn_3N$ and found the reason for this M_S reduction. The details will be explained elsewhere.

Figures 4(a) and 4(b) show torque curves of Mn_4N and $Co_{0.2}Mn_{3.8}N$ films measured at RT under various H values. θ is the angle between H and the plane of the film; $\theta = 0°$ means that H is applied in parallel to $Co_xMn_{4-x}N[100]$, the in-plane direction, and $\theta = 90°$ shows that H is parallel to $Co_xMn_{4-x}N[001]$, normal to the sample surface. These curves exhibit two-hold symmetry because of PMA. The amplitude of the torque curves increases with increasing H, whereas the hysteresis loss observed around $\theta = 0°$ and 180° is reduced. Since the hysteresis loss is observed even at 25 kOe, H_k is greater than 25 kOe in both samples. This result is consistent with the results shown in Fig. 3. The sawtooth-like curves show that the magnetization was not saturated. Since the magnetization direction was not parallel to H, K_u values were underestimated when we derived them from the maximum amplitude of the torque curves. Thus, we used the 45°-torque method to estimate K_u from unsaturated magnetic torque curves. Figure 4(c) shows the $(T/H)^2$ –T plots using the averaging-out absolute values at $\theta = 45°$, 135°, 225°, and 315°. The M_S and K_u^{eff} values were obtained from the intersections of the fitting lines with the vertical and horizontal axes, respectively.[20] Using the equation $K_u = K_u^{eff} + 2\pi M_S^2$, the K_u values were calculated to be 1.0×10^6 and 8.9×10^5 erg/cm^3 for Mn_4N and $Co_{0.2}Mn_{3.8}N$, respectively. This result shows that the addition of a small amount of Co into Mn_4N decreased both M_S and K_u. The obtained K_u for Mn_4N is comparable

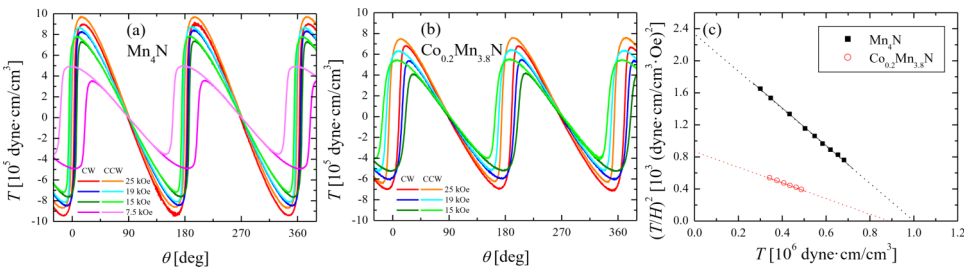

FIG. 4. Magnetic torque curves of (a) Mn_4N and (b) $Co_{0.2}Mn_{3.8}N$ films measured at RT under various H values. (c) $(T/H)^2$ versus T plots.

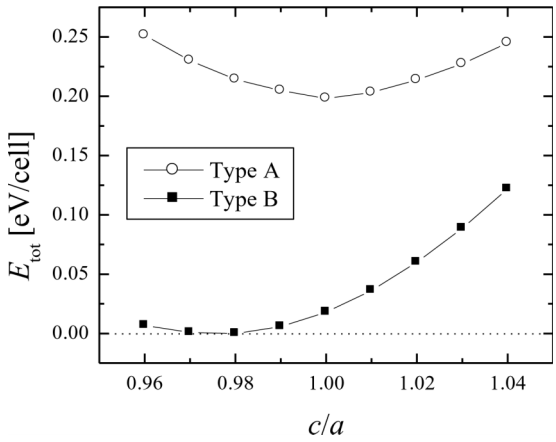

FIG. 5. E_{tot} versus c/a plots in type A and B Mn_4N.

TABLE I. First-principles calculation results for Mn_4N.

Type	E_{tot} [eV/cell]	a, c [nm]	m_{spin} [μ_B per atom] I site	IIA site	IIB site	N	M_S [emu/cm^3]
A	0.20	0.3870 ($c/a = 1.00$)	3.898	−1.678	−1.678	0.109	164
B	0	0.3896(a) 0.3818(c) ($c/a = 0.98$)	3.618	−2.749	0.944	0.014	147

to those reported for Mn_4N on MgO(001) grown by PLD (1.6×10^6 erg/cm^3) determined from the magnetization measurement,[17] and that grown by sputtering (8.8×10^5 erg/cm^3) determined from magnetic torque measurement.[19]

We next discuss the calculation results. Figure 5 shows the E_{tot} versus c/a plots in both type A and B Mn_4N. Here, E_{tot} was compared with respect to type B Mn_4N with $c/a = 0.98$. E_{tot} of type A and B Mn_4N reached a minimum at $c/a = 1.00$ and 0.98, respectively, and E_{tot} of type A Mn_4N are higher than that of type B. This means that the type B Mn_4N with the tetragonal structure of $c/a = 0.98$ is predicted to be an energetically stable phase. Table I shows the lattice constants a and c, m_{spin} of each site, and M_S in the type A and B Mn_4N when their E_{tot}'s show a minimum. Calculated M_S of the type B Mn_4N was slightly smaller than those of the type A and bulk[3] but close to those reported for Mn_4N films.[15–19] Tetragonal-structured Mn atoms (fct-Mn), possessing the anti-ferromagnetic configuration similar to that of type B Mn_4N, was confirmed both experimentally ($c/a = 0.945$)[25] and theoretically ($c/a = 0.90$).[26] It might be possible that intrinsic tetragonal Mn_4N was realized by the same mechanism as that of fct-Mn described in Ref. 26. On the other hand, the bulk Mn_4N possesses cubic structure[3] and it seems to be inconsistent with our calculated results. However, we assumed the collinear ferrimagnetic configuration on the calculation of Mn_4N, and we should note that there are several reports on the non-collinear ferrimagnetic configuration of bulk Mn_4N.[27,28] We consider that the formation of the intrinsic tetragonal ($c/a < 1$) Mn_4N phase is probable when Mn_4N films are epitaxially grown on the substrates, which have a larger lattice constant than that of the bulk Mn_4N. Actually, $c/a < 1$ and PMA were reported in the Mn_4N films grown on MgO(001) ($a = 0.421$ nm) and STO(001) ($a = 0.391$ nm) substrates having larger lattice constants.[15–19]

IV. CONCLUSION

We grew approximately 25-nm-thick Mn_4N and $Co_{0.2}Mn_{3.8}N$ epitaxial thin films on STO(001) substrates by MBE. Both samples showed PMA, and M_S values were 80 and 60 emu/cm^3,

respectively, at 300 K. The ratio $c/a \sim 0.99$ was confirmed from the x-ray reciprocal lattice mapping. The K_u values determined from the magnetic torque measurement were 1.0×10^6 and 8.9×10^5 erg/cm^3, respectively. H_k value increased, and both K_u and M_S values decreased as the Co composition increased. The first-principles calculations suggested that there is the intrinsic tetragonal Mn_4N. This explains the reason why the $c/a \sim 0.99$ was reported in the Mn_4N films epitaxially grown on MgO(001) and STO(001) substrates regardless of the Mn_4N film thickness and lattice mismatch on these substrates.

ACKNOWLEDGMENTS

This work was financially supported in part by Grants-in-Aid for JSPS Fellows (No. 14J01804), Scientific Research (A) (No. 26249037) from JSPS, and the Cooperative Research Project (H26/A04) from the Research Institute of Electric Communication, Tohoku University. Magnetization curve measurements were performed with the help of Mr. R. Ishikawa, Dr. H. Oikawa, Dr. R. Akiyama, and professor S. Kuroda of the University of Tsukuba. We thank professor T. Oguchi of Osaka University for his advice.

[1] K. Miura, T. Kawahara, R. Takemura, J. Hayakawa, S. Ikeda, R. Sasaki, H. Takahashi, H. Matsuoka, and H. Ohno, in *Proc. Int. Symp. VLSI Technology* (2007), p. 234.
[2] S. S. P. Parkin, M. Hayashi, and L. Thomas, Science **320**, 190 (2008).
[3] W. J. Takei, R. R. Heikes, and G. Shirane, Phys. Rev. **125**, 1893 (1962).
[4] F. Li, J. Yang, D. Xue, and R. Zhou, Appl. Phys. Lett. **66**, 2343 (1995).
[5] I. Pop, R. Muntean, and O. Pop, Materials Letters **28**, 155 (1996).
[6] S. Kokado, N. Fujima, K. Harigaya, H. Shimizu, and A. Sakuma, Phys. Rev. B **73**, 172410 (2006).
[7] M. S. Patwari and R. H. Victora, Phys. Rev. B **64**, 214417 (2006).
[8] K. Ito, G. H. Lee, H. Akinaga, and T. Suemasu, J. Cryst. Growth **322**, 63 (2011).
[9] Y. Takahashi, Y. Imai, and T. Kumagai, J. Magn. Magn. Mater. **323**, 2941 (2011).
[10] P. Monachesi, T. Björkman, T. Gasche, and O. Eriksson, Phys. Rev. B **88**, 054420 (2013).
[11] K. Ito, T. Sanai, Y. Yasutomi, S. Zhu, K. Toko, Y. Takeda, Y. Saitoh, A. Kimura, and T. Suemasu, J. App. Phys. **115**, 17C712 (2014).
[12] H. Sakakibara, H. Ando, Y. Kuroki, S. Kawai, K. Ueda, and H. Asano, J. App. Phys. **117**, 17D725 (2015).
[13] K. M. Ching, W. D Chang, and T. S. Chin, J. Alloys. Compd. **222**, 184 (1995).
[14] K. M. Ching, W. D. Chang, T. S. Chin, J. G. Duh, and H. C. Ku, J. Appl. Phys. **76**, 6582 (1994).
[15] M. Tsunoda and K. Kabara, in *International Conference of the Asian Union of Magnetics Societies (ICAUMS)* (The AUMS, Nara, 2012), p. 2pPS-47.
[16] Y. Yasutomi, K. Ito, T. Sanai, K. Toko, and T. Suemasu, J. Appl. Phys. **115**, 17A935 (2014).
[17] X. Shen, A. Chikamatsu, K. Shigematsu, Y. Hirose, T. Fukumura, and T. Hasegawa, Appl. Phys. Lett. **105**, 072410 (2014).
[18] M. Meng, S. X. Wu, L. Z. Ren, W. Q. Zhou, Y. J. Wang, G. L. Wang, and S. W. Li, Appl. Phys. Lett. **106**, 032407 (2015).
[19] K. Kabara and M. Tsunoda, J. Appl. Phys. **117**, 17B512 (2015).
[20] H. Miyajima, K. Sato, and T. Mizoguchi, J. Appl. Phys. **47**, 4669 (1976).
[21] G. Henkelman, A. Arnaldsson, and H. Jonsson, Comput. Mater. Sci. **36**, 354 (2006).
[22] G. Kresse and D. Joubert, Phys. Rev. B **59**, 1758 (1999).
[23] P. E. Blöchl, Phys. Rev. B **50**, 17953 (1994).
[24] J. P. Perdew and Y. Wang, Phys. Rev. B **33**, 8800 (1986).
[25] Y. Endoh and Y. Ishikawa, J. Phys. Soc. Jpn. **30**, 1614 (1971).
[26] T. Oguchi and A. J. Freeman, J. Magn. Magn. Mater. **46**, L1 (1984).
[27] D. Fruchart, D. Givord, P. Convert, P. L'Heritiers, and J. P. Senateur, J. Phys. F **9**, 2431 (1979).
[28] M. Uhl, S. F. Matar, and P. Mohn, Phys. Rev. B **55**, 2995 (1997).